ISSN 2218-4333 (online)

World Journal of *Clinical Oncology*

World J Clin Oncol 2021 September 24; 12(9): 712-832

Published by Baishideng Publishing Group Inc

WJCO

World Journal of Clinical Oncology

Contents

Monthly Volume 12 Number 9 September 24, 2021

REVIEW

712 Embracing cancer immunotherapy with vital micronutrients

Yuen RCF, Tsao SY

725 Metastatic disease to the liver: Locoregional therapy strategies and outcomes

Zane KE, Cloyd JM, Mumtaz KS, Wadhwa V, Makary MS

746 Hematopoietic stem cell mobilization strategies to support high-dose chemotherapy: A focus on relapsed/refractory germ cell tumors

Porfyriou E, Letsa S, Kosmas C

767 Re-irradiation for high-grade gliomas: Has anything changed?

García-Cabezas S, Rivin del Campo E, Solivera-Vela J, Palacios-Eito A

MINIREVIEWS

787 Real-world evidence on first- and second-line palliative chemotherapy in advanced pancreatic cancer

Blomstrand H, Batra A, Cheung WY, Elander NO

ORIGINAL ARTICLE

Retrospective Cohort Study

800 Long-term results of the treatment of Hodgkin's lymphoma in a resource-constrained setting: Real-world data from a single center

Sánchez-Valledor LF, Habermann TM, Murrieta-Alvarez I, Córdova-Ramírez AC, Rivera-Álvarez M, León-Peña A, Cantero-Fortiz Y, Olivares-Gazca JC, Ruiz-Delgado GJ, Ruiz-Argüelles GJ

Retrospective Study

808 Role of mammogram and ultrasound imaging in predicting breast cancer subtypes in screening and symptomatic patients

Ian TWM, Tan EY, Chotai N

823 Features of primary pancreatic lymphoma: A bi-institutional review with an emphasis on typical and atypical imaging features

Segaran N, Sandrasegaran K, Devine C, Wang MX, Shah C, Ganeshan D

World Journal of Clinical Oncology

Monthly Volume 12 Number 9 September 24, 2021

Contents

ABOUT COVER

Editorial Board Member of *World Journal of Clinical Oncology*, Dhakshina Ganeshan, MD, Associate Professor, Department of Abdominal Imaging, Division of Diagnostic Imaging, The University of Texas MD Anderson Cancer Center, 1515 Holcombe Blvd, Houston, TX 77030, United States. dganeshan@mdanderson.org

AIMS AND SCOPE

The primary aim of *World Journal of Clinical Oncology* (*WJCO*, *World J Clin Oncol*) is to provide scholars and readers from various fields of oncology with a platform to publish high-quality basic and clinical research articles and communicate their research findings online.

WJCO mainly publishes articles reporting research results and findings obtained in the field of oncology and covering a wide range of topics including art of oncology, biology of neoplasia, breast cancer, cancer prevention and control, cancer-related complications, diagnosis in oncology, gastrointestinal cancer, genetic testing for cancer, gynecologic cancer, head and neck cancer, hematologic malignancy, lung cancer, melanoma, molecular oncology, neurooncology, palliative and supportive care, pediatric oncology, surgical oncology, translational oncology, and urologic oncology.

INDEXING/ABSTRACTING

The *WJCO* is now abstracted and indexed in PubMed, PubMed Central, Emerging Sources Citation Index (Web of Science), China National Knowledge Infrastructure (CNKI), China Science and Technology Journal Database (CSTJ), and Superstar Journals Database. The 2021 edition of Journal Citation Reports® cites the 2020 Journal Citation Indicator (JCI) for *WJCO* as 0.48.

RESPONSIBLE EDITORS FOR THIS ISSUE

NAME OF JOURNAL
World Journal of Clinical Oncology

ISSN
ISSN 2218-4333 (online)

LAUNCH DATE
November 10, 2010

FREQUENCY
Monthly

EDITORS-IN-CHIEF
Hiten RH Patel, Stephen Safe

EDITORIAL BOARD MEMBERS
https://www.wjgnet.com/2218-4333/editorialboard.htm

PUBLICATION DATE
September 24, 2021

INSTRUCTIONS TO AUTHORS
https://www.wjgnet.com/bpg/gerinfo/204

GUIDELINES FOR ETHICS DOCUMENTS
https://www.wjgnet.com/bpg/GerInfo/287

GUIDELINES FOR NON-NATIVE SPEAKERS OF ENGLISH
https://www.wjgnet.com/bpg/gerinfo/240

PUBLICATION ETHICS
https://www.wjgnet.com/bpg/GerInfo/288

PUBLICATION MISCONDUCT
https://www.wjgnet.com/bpg/gerinfo/208

ARTICLE PROCESSING CHARGE
https://www.wjgnet.com/bpg/gerinfo/242

STEPS FOR SUBMITTING MANUSCRIPTS
https://www.wjgnet.com/bpg/GerInfo/239

ONLINE SUBMISSION
https://www.f6publishing.com

World Journal of Clinical Oncology

Submit a Manuscript: https://www.f6publishing.com

World J Clin Oncol 2021 September 24; 12(9): 808-822

DOI: 10.5306/wjco.v12.i9.808

ISSN 2218-4333 (online)

ORIGINAL ARTICLE

Retrospective Study

Role of mammogram and ultrasound imaging in predicting breast cancer subtypes in screening and symptomatic patients

Tay Wei Ming Ian, Ern Yu Tan, Niketa Chotai

ORCID number: Tay Wei Ming Ian 0000-0003-0401-1420; Ern Yu Tan 0000-0001-7726-3974; Niketa Chotai 0000-0003-4005-2123.

Author contributions: Ian TWM contributed to data collection, statistical analysis, and manuscript writing; Tan EY contributed to data collection and ethics committee approval application; Chotai N contributed to data collection and manuscript editing.

Institutional review board statement: The Institutional review board was approved by the NHG DSRB, DSRB Reference Number: 2019/00058.

Informed consent statement: The Informed consent statement was waived by the Institutional review board.

Conflict-of-interest statement: The authors have stated that they have no conflicts of interest.

Data sharing statement: Technical appendix, statistical code, and dataset available from the corresponding author at niketachotai@gmail.com. Participants gave informed consent for data sharing as part of their inclusion into the hospital breast cancer registry.

Tay Wei Ming Ian, Department of Diagnostic Radiology, Singapore General Hospital, Singapore 101070, Singapore

Ern Yu Tan, Department of General Surgery, Tan Tock Seng Hospital, Singapore 308433, Singapore

Niketa Chotai, Department of Diagnostic Radiology, Tan Tock Seng Hospital, Singapore 308433, Singapore

Corresponding author: Niketa Chotai, MBBS, MD, Academic Research, Attending Doctor, Department of Diagnostic Radiology, Tan Tock Seng Hospital, 11 Jalan Tan Tock Seng, Singapore 308433, Singapore. niketachotai@gmail.com

Abstract

BACKGROUND

Breast cancer (BC) radiogenomics, or correlation analysis of imaging features and BC molecular subtypes, can complement genetic analysis with less resource-intensive diagnostic methods to provide an early and accurate triage of BC. This is pertinent because BC is the most prevalent cancer amongst adult women, resulting in rising demands on public health resources.

AIM

To find combinations of mammogram and ultrasound imaging features that predict BC molecular subtypes in a sample of screening and symptomatic patients.

METHODS

This retrospective study evaluated 328 consecutive patients in 2017-2018 with histologically confirmed BC, of which 237 (72%) presented with symptoms and 91 (28%) were detected *via* a screening program. All the patients underwent mammography and ultrasound imaging prior to biopsy. The images were retrospectively read by two breast-imaging radiologists with 5-10 years of experience with no knowledge of the histology results to ensure statistical independence. To test the hypothesis that imaging features are correlated with tumor subtypes, univariate binomial and multinomial logistic regression models were performed. Our study also used the multivariate logistic regression (with and without interaction terms) to identify combinations of mammogram and ultrasound (US) imaging characteristics predictive of molecular subtypes.

Manuscript source: Unsolicited manuscript

Specialty type: Radiology, nuclear medicine and medical imaging

Country/Territory of origin: Singapore

Peer-review report's scientific quality classification

Grade A (Excellent): 0
Grade B (Very good): 0
Grade C (Good): C, C
Grade D (Fair): 0
Grade E (Poor): 0

Received: February 23, 2021
Peer-review started: February 23, 2021
First decision: June 16, 2021
Revised: June 24, 2021
Accepted: August 3, 2021
Article in press: August 3, 2021
Published online: September 24, 2021

P-Reviewer: Bansal C
S-Editor: Zhang H
L-Editor: Filipodia
P-Editor: Guo X

RESULTS

The presence of circumscribed margins, posterior enhancement, and large size is correlated with triple-negative BC (TNBC), while high-risk microcalcifications and microlobulated margins is predictive of HER2-enriched cancers. Ductal carcinoma *in situ* is characterized by small size on ultrasound, absence of posterior acoustic features, and architectural distortion on mammogram, while luminal subtypes tend to be small, with spiculated margins and posterior acoustic shadowing (Luminal A type). These results are broadly consistent with findings from prior studies. In addition, we also find that US size signals a higher odds ratio for TNBC if presented during screening. As TNBC tends to display sonographic features such as circumscribed margins and posterior enhancement, resulting in visual similarity with benign common lesions, at the screening stage, size may be a useful factor in deciding whether to recommend a biopsy.

CONCLUSION

Several imaging features were shown to be independent variables predicting molecular subtypes of BC. Knowledge of such correlations could help clinicians stratify BC patients, possibly enabling earlier treatment or aiding in therapeutic decisions in countries where receptor testing is not readily available.

Key Words: Hormone receptor; Molecular subtype; Ultrasonography; Mammography; Triple-negative cancer; Breast cancer screening

Core Tip: Ultrasound and mammogram imaging features are correlated with breast cancer (BC) molecular subtypes. Knowledge of such correlations helps clinicians stratify patients, enabling earlier treatment or aiding therapeutic decisions. In a sample of symptomatic and asymptomatic (screening) patients, multivariate logistic regression showed that a combination of imaging features can distinguish: (1) Hormone receptor positive *vs* hormone receptor negative; (2) Triple negative BC (TNBC) *vs* non-TNBC; and (3) HER2+ (human epidermal receptor positive) *vs* non-HER2+ BC.

Citation: Ian TWM, Tan EY, Chotai N. Role of mammogram and ultrasound imaging in predicting breast cancer subtypes in screening and symptomatic patients. *World J Clin Oncol* 2021; 12(9): 808-822
URL: https://www.wjgnet.com/2218-4333/full/v12/i9/808.htm
DOI: https://dx.doi.org/10.5306/wjco.v12.i9.808

INTRODUCTION

Breast cancer (BC) radiogenomics has been a prolific field of research in recent years, with an expanding number of studies examining the extent to which imaging can be utilized as a screening adjunct in the preliminary diagnosis of BC molecular subtypes [1]. While magnetic resonance imaging (MRI) has been the mainstay of radiogenomics, as it can produce a wide range of imaging features, a few studies have also utilized readily available modalities, such as mammogram (MG) and hand-guided ultrasound (US). These highlight the advantages of using cost-effective imaging tools that can be used for an early and accurate diagnosis of the cancer subtype[2].

The use of non-invasive, less resource-intensive methods to predict BC subtypes has practical significance, for two reasons. First, as BC is the most common cancer amongst adult women in the world, leveraging on radiologic imaging as a proxy for expensive genetic tests may help to lower the public health burden, particularly in the context of less developed countries where detailed and costly histopathologic analysis is not readily available. Second, BC is a heterogeneous disease—receptor expression and gene amplification profiles have different prognoses for disease progression and therapeutic response. Thus, radiologic imaging as an adjunct to genetic profiling can assist in pre-treatment planning and provide an additional level of analysis for radio-pathologic correlation discussions.

Prior research has established some degree of consensus regarding the correlation of imaging features with BC subtype, with ultrasound margins, posterior acoustic features, and high-risk microcalcifications (on MG) found to be independent imaging differentiators between molecular subtypes[3].

While previous studies focused mainly on symptomatic patients, this study aims to analyze which combination of US and MG imaging features are the most predictive of molecular subtypes in a patient population that comprises both symptomatic and asymptomatic (breast screening) patients. A unique feature of our dataset is a substantial proportion—slightly under 30% of the patients in our sample patients had cancers detected *via* our national screening program (91 of 328, 28%). This allows us to examine if imaging features indicative of higher-grade cancers can be detected in asymptomatic patients who undergo routine screening checks. In addition, due to the inclusion of screening patients, a significant proportion of cancers detected in our sample included non-invasive ductal carcinoma *in situ* (DCIS) (or 53 of 328, 16%). Thus, we were also able to analyze its mammographic and sonographic characteristics in relation to the four subtypes of invasive BCs, which to the best of our knowledge, has not been published in the existing literature.

MATERIALS AND METHODS

Patient data and selection criteria

Approval for this study was obtained from the local institutional review board. The need for informed consent for this study was waived due to the retrospective design, as patients had given permission to be included in the hospital's BC registry and the use of their unidentified data for research.

To minimize selection bias, our sample included consecutive patients with histologically confirmed BC diagnosed from January 2017 to December 2018. The surgical notes, histology reports, and medical images of 328 patients were retrieved *via* the hospital's electronic medical record system. The images were retrospectively read by two breast-imaging radiologists with 5-10 years of experience with no knowledge of the histology results to ensure statistical independence with regards to the dependent variable(s).

Imaging equipment and assessment

Standard two-view digital mammography was performed, with additional views when necessary, using Fuji or GE mammography units. Mammograms were interpreted by two breast imaging radiologists who were blinded to the histopathology report. Following the American College of Radiology (ACR) Breast Imaging Reporting and Data System (BI-RADS) reporting lexicon, abnormal mammographic findings were classified as an asymmetry, mass, architectural distortion, or suspicious microcalcifications.

Breast ultrasound was performed by ultrasound technologists using 12-5 Mhz transducers, with images interpreted by two breast imaging radiologists who were blinded to the histopathology report. Final decisions were made with consensus agreement among the radiologists. Each tumor was measured in three planes, with color Doppler images also acquired. Following the ACR BI-RADS guidelines, the lesion's margins, echogenicity, posterior features, and vascularity (Adler's index) were documented, along with size on ultrasound (Table 1).

Immunochemistry and classification of molecular subtypes

The expression status of the ER, PR, and HER2 receptors was assessed using an avidin-biotin complex immunohistochemical technique. The ER/PR statuses were evaluated using the Allred score based on the proportion of positively stained nuclei. Allred scores of at least 3 were considered as hormone receptor positive (ER+/PR+). The HER2 staining intensity was scored from 0 to 3+. Scores of 3+ were classified as HER2 positive (HER2+), whereas scores of 0/1+ were considered as HER2 negative (HER2-). Tumors with scores of 2+ were further assessed with fluorescence *in situ* hybridization to determine their HER2 status. The threshold ratio of the HER2 gene signal to the chromosome 17 probe signal was 2.2, above which the tumor was classified as HER2+ and below which the tumor was classified as HER2-.

For this paper, we have classified Luminal A tumors as being ER+/PR+ and HER2-, Luminal B tumors as being ER+/PR+ and HER2+, HER2-enriched as ER-/PR- and HER2+, and triple negative BC (TNBC) as being ER-/PR- and HER2-.

Table 1 Classification of imaging features based on American College of Radiology Breast Imaging Reporting and Data System Lexicon

Imaging feature	Classification
Mammogram	
Appearance	Mass
	Asymmetry
	High risk microcalcifications[1]
	Architectural distortion
Ultrasound	
Margins	Spiculated
	Microlobulated
	Circumscribed
Posterior acoustic features	Shadowing
	Enhancement
	Mixed
	None
Size	Maximum dimension on ultrasound (in mm)
Echogenicity	Homogenous
	Heterogeneous
	Complex cystic
Adler's index	Low (Grade I)
	Medium (Grade II)
	High (Grade III)

[1]High risk microcalcifications refer to microcalcifications which show grouped, linear, or segmental distribution, or with a pleomorphic or branching morphology.

Statistical analysis

Descriptive statistics were generated for the 328 patients included in the study. Clinicopathologic, mammogram, and ultrasound characteristics were based on the ACR BI-RADS lexicon. Data was summarized using frequency and percentage for qualitative variables, mean ± SD, and range for quantitative variables, as listed in Table 2.

To test the primary hypothesis that imaging features are correlated with tumor subtypes, univariate binomial and multinomial logistic regression models were performed. Our study also used the multivariate logistic regression (with and without interaction terms), to assess if a joint combination of MG and US imaging characteristics is predictive of molecular subtypes, and the results are summarized in Tables 3-6. The specification for the multivariate model was derived using stepwise regression (SLE = 0.05, SLS = 0.05). Discrimination and classification of the final multivariate models or predictor were assessed using the area under the receiver operating characteristic curve (AUC). All analysis was performed with the use of statistical software (RStudio, Version 1.3.1073), using the mlogit (v.1.1-0; Croissant, 2002), nnet (v2.13.1; Venables & Ripley, 2002)[4,5], and pROC (Robin *et al*[6]) packages.

RESULTS

Out of the 328 cases, 139 (48%) were ER+/PR+, HER2- (Luminal A type); 38 (12%) were ER+/PR+, HER2+ (Luminal B type); 50 (15%) were ER-/PR-, HER2+ (HER2-enriched type); 48 (15%) were ER-/PR-, HER2- (triple negative type), and 53 (16%) were DCIS. The age range of the study sample was 31-86-years-old, with a mean age of 61.1 years. Across the four molecular subtypes, there was no significant difference in age. Ninety-one (27%) cases were detected *via* breast screening, while the remaining

Table 2 Distribution of demographic and imaging parameters based on molecular subtype

	Total (*n* = 328)	DCIS (*n* = 53)	Luminal A (*n* = 139)	Luminal B (*n* = 38)	Her2 enriched (*n* = 50)	Triple negative (*n* = 48)
Mean age	61.1 ± 11.75	59.1 ± 11.67	61.8 ± 11.80	60.2 ± 12.23	62.0 ± 9.63	61.3 ± 12.60
Presentation						
Clinic	237 (72%)	29 (55%)	98 (71%)	28 (74%)	36 (72%)	46 (96%)
Screening	91 (28%)	24 (45%)	41 (29%)	10 (26%)	14 (28%)	2 (4%)
Mass	200 (61%)	14 (26%)	91 (65%)	29 (76%)	29 (58%)	37 (77%)
Architectural distortion	17 (6%)	7 (13%)	10 (7%)	0 (0%)	0 (0%)	0 (0%)
Asymmetry	40 (12%)	6 (11%)	16 (12%)	3 (8%)	9 (18%)	6 (13%)
High-risk microcalcifications	105 (32%)	27 (51%)	33 (24%)	12 (32%)	24 (48%)	9 (19%)
Tumor size (on USG)						
< 20	136 (41%)	22 (42%)	71 (51%)	20 (53%)	19 (38%)	4 (8%)
≥ 20	154 (47%)	9 (17%)	55 (40%)	17 (45%)	29 (58%)	44 (92%)
Margins (on USG)						
Spiculated	100 (30%)	5 (9%)	63 (45%)	12 (32%)	8 (16%)	8 (17%)
Microlobulated	174 (60%)	23 (43%)	59 (42%)	25 (66%)	40 (80%)	29 (60%)
Circumscribed	16 (5%)	3 (6%)	4 (3%)	0 (0%)	0 (0%)	11 (23%)
Echogenicity (on USG)						
Heterogeneous	144 (44%)	13 (25%)	58 (42%)	19 (50%)	28 (56%)	26 (54%)
Homogenous	146 (45%)	18 (34%)	68 (49%)	18 (47%)	20 (40%)	22 (46%)
Posterior acoustic features						
Shadow	74 (23%)	5 (9%)	49 (35%)	10 (26%)	4 (8%)	6 (13%)
Enhancement	85 (26%)	5 (9%)	23 (17%)	8 (21%)	6 (32%)	33 (69%)
Mixed	36 (11%)	5 (9%)	15 (11%)	3 (8%)	9 (18%)	4 (8%)
None	95 (29%)	16 (30%)	39 (28%)	16 (42%)	19 (38%)	5 (10%)
Adler's vascularity						
High (Grade II & III)	81 (25%)	7 (13%)	22 (16%)	11 (29%)	21 (42%)	20 (42%)
Low (Grade I)	209 (64%)	24 (45%)	104 (75%)	26 (68%)	27 (54%)	28 (58%)
Axillary nodes						
Present	56 (17%)	0 (0%)	25 (18%)	1 (3%)	14 (28%)	16 (33%)
Absent	234 (71%)	53 (100%)	101 (73%)	36 (95%)	34 (68%)	32 (67%)
Not visible on US	38 (14%)	22 (42%)	13 (9%)	1 (3%)	2 (1%)	0 (0%)

DCIS: Ductal carcinoma *in situ*; US: Ultrasound; USG: Ultrasonography.

191 (69%) cases presented with symptoms at the breast clinic. Most of the cases (89%) detected *via* breast screening were classified as DCIS or hormone receptor positive cancer, and only a minority (11%) of cases detected *via* screening were hormone receptor negative cancers.

Microcalcifications

High risk microcalcifications were found in slightly under one third of the full sample (n = 105, 32%) but were more prevalent amongst BC patients with the subtype HER2-enriched (n = 24, 48%) and DCIS (n = 27, 51%) (Figure 1A). In the univariate multinomial logistic regression (with reference to Luminal A as the baseline), the presence of high risk microcalcifications on mammography was positively associated

Table 3 Binomial univariate and multivariate logistic regressions (ER/PR positive *vs* negative)

ER/PR positive *vs* negative		Univariate			Multivariate (AUC = 0.792)		
		P	OR	CI	*P*	OR	CI
Posterior acoustic features[1]	Enhancement	[d]	0.46	(0.193 1.050)	[d]	0.45	(0.174 1.143)
	Shadowing	[b]	4.26	(1.617 11.633)	Not significant		
Margins[2]	Spiculated	[a]	4.16	(2.268 7.975)	[a]	0.41	(1.085 4.606)
	Circumscribed	[a]	0.15	(0.023 0.594)	Not significant		
Size	Small < 20 mm	[c]	4.51	(2.499 7.443)	[a]	2.74	(1.475 5.204)

[1]Mixed posterior acoustic features were set as the baseline with OR = 1.
[2]Microlobulated ultrasound margins were set as the baseline with OR = 1.
[a]Significant at the 0.001 level.
[b]Significant at the 0.01 level.
[c]Significant at the 0.05 level.
[d]Significant at the 0.10 level.
Area under the receiver operating characteristic curve for multivariate regression on posterior acoustic features, ultrasound margins, MM high-risk microcalcifications, and size (large or small).

Table 4 Binomial univariate and multivariate logistic regressions (Triple-negative breast cancer *vs* Non-triple-negative breast cancer)

TNBC *vs* Non-TNBC		Univariate			Multivariate (AUC = 0.853)		
		P	OR	CI	*P*	OR	CI
Posterior acoustic features[1]	Enhancement	[b]	5.08	(1.808 18.201)	[a]	4.77	(1.556 18.291)
Margins[2]	Spiculated	[a]	0.43	(0.179 0.951)	Not significant		
	Circumscribed	[c]	11.00	(3.712 37.166)	[b]	8.24	(2.151 38.923)
Size	Large > 20 mm	[c]	13.2	(5.152 44.845)	[c]	10.5	(3.792 38.436)
Axillary node metastasis	Yes	[b]	2.52	(1.247 4.988)	Not significant		
Adler's Index	High	[a]	2.12	(1.104 4.020)	Not significant		
[a]Screening	Yes	[d]	0.003	(0.000 0.222)	[d]	0.004	(0.000 0.452)
[a]Interaction term	Screen × unit size	[d]	1.17	(1.003 1.505)	[d]	1.16	(1.001 1.430)

[1]Mixed posterior acoustic features were set as the baseline with OR = 1.
[2]Microlobulated ultrasound margins were set as the baseline with OR = 1.
[a]Significant at the 0.001 level.
[b]Significant at the 0.01 level.
[c]Significant at the 0.05 level.
[d]Significant at the 0.10 level.
Area under the receiver operating characteristic curve for multivariate regression on posterior acoustic features, ultrasound margins, and size (large or small). AUC: Area under the receiver operating characteristic curve; TNBC: Triple-negative breast cancer.

with the presence of HER2 receptor expression (P = 0.002, OR 2.97) and DCIS ($P \leq$ 0.001, OR 3.34). In the multivariate logistic regression, high-risk microcalcifications also increase the relative odds of the tumor being a HER2-enriched type ($P \leq$ 0.001, OR 3.38) (Table 5).

Architectural distortions

Architectural distortions presented rarely in DCIS (n = 7, 13%) and Luminal A subtypes (n = 10, 7%), and were not common in the other three subtypes of BC. On univariate analysis, architectural distortions were significantly associated with DCIS (P = 0.024, OR 3.23) (Table 6), but no statistically significant relationship with Luminal A type was found.

Margins

The vast majority of tumors in our study (n = 274, 94%) had non-circumscribed

Table 5 Binomial univariate and multivariate logistic regressions (HER2+ *vs* Non HER2+)

HER2+ *vs* Non HER2+		Univariate			Multivariate (AUC = 0.747)		
		P	OR	CI	*P*	OR	CI
Margins[1]	Microlobulated	[c]	3.92	(1.830 9.410)	[b]	3.26	(1.469 8.026)
	Circumscribed	Not significant			Not significant		
High-risk microcalcifications	Present	[c]	3.51	(1.804 6.821)	[c]	3.38	(1.685 6.816)
Adler's Index	High	[a]	2.32	(1.203 4.437)	[a]	1.99	(0.999 4.010)

[1]Spiculated ultrasound margins were set as the baseline with OR = 1.
[a]Significant at the 0.001 level.
[b]Significant at the 0.01 level.
[c]Significant at the 0.05 level.
[d]Significant at the 0.10 level.
Area under the receiver operating characteristic curve for multivariate regression on ultrasound (US) margins, MM high-risk microcalcifications, and US Adler index (low or intermediate/high). AUC: Area under the receiver operating characteristic curve.

Table 6 Binomial univariate and multivariate logistic regressions (Ductal carcinoma *in situ* *vs* Invasive cancers)

DCIS *vs* Invasive cancers		Univariate			Multivariate (AUC = 0.719)		
		P	OR	CI	*P*	OR	CI
Posterior acoustic features[1]	None	[a]	3.24	(1.204 10.292)	[a]	3.45	(1.255 11.118)
High-risk microcalcifications	Present	[b]	2.80	(1.516 5.208)	Not significant		
Architectural distortions	Yes	[b]	5.34	(1.546 16.709)	Not significant		
Size	Small < 20 mm	[a]	2.59	(1.420 7.361)	[a]	2.72	(1.172 6.182)

[1]Posterior acoustic enhancement was set as the baseline with OR = 1.
[a]Significant at the 0.001 level.
[b]Significant at the 0.01 level.
[c]Significant at the 0.05 level.
[d]Significant at the 0.10 level.
Area under the receiver operating characteristic curve for multivariate regression on posterior acoustic features, MM high-risk microcalcifications, architectural distortions, and size (large or small). AUC: Area under the receiver operating characteristic curve; DCIS: Ductal carcinoma *in situ*.

margins, of which more than half were classified as microlobulated (n = 174, 60%), followed by spiculated margins (n = 100, 34%). Only 6% of all lesions showed circumscribed margins, of which the majority were TNBC cases (n = 11, 4%), and the rest were DCIS (n = 3, 1%). Based on the univariate and multivariate logistic regressions, the presence of circumscribed margins was found to significantly increase the relative odds of TNBC cancer (univariate: P = 0.003, OR 11.0; multivariate: P = 0.004, OR 8.24) (Figure 2A, Table 4). Moreover, the presence of a spiculated margin on sonography was common in Luminal A cancers (n = 67, 53%), but rarely presented in TN and HER2+ tumors (n = 16, 16%). Thus, if the tumor shows spiculated margins, the odds of it being a hormone receptor positive subtype is higher, as confirmed in the univariate and multivariate regressions (univariate: P = 0.000, OR 4.16; multivariate: P = 0.03, OR 2.20) (Table 3).

Posterior acoustic features

Posterior acoustic enhancement was more common in HER2-enriched and TN tumors (n = 16, 32% and n = 33, 69%), compared to luminal cancers (n = 31, 19%) and DCIS (n = 5, 9%). It is a strong predictor for TNBC cancers *vs* non-TNBC cancers (univariate: P = 0.005 OR 5.08; multivariate: P = 0.01 OR 4.77) (Figure 2B, Table 4). In the multinomial logistic regressions, posterior enhancement signaled higher relative odds of the tumor being a TNBC cancer relative to Luminal A, DCIS, and HER2-enriched tumors (Table 4).

Conversely, posterior acoustic shadowing is associated with slightly higher odds of the tumor being a hormone positive type. In Luminal A cancers, posterior shadowing (n = 49, 39%) was more prevalent compared to the other three subtypes of invasive

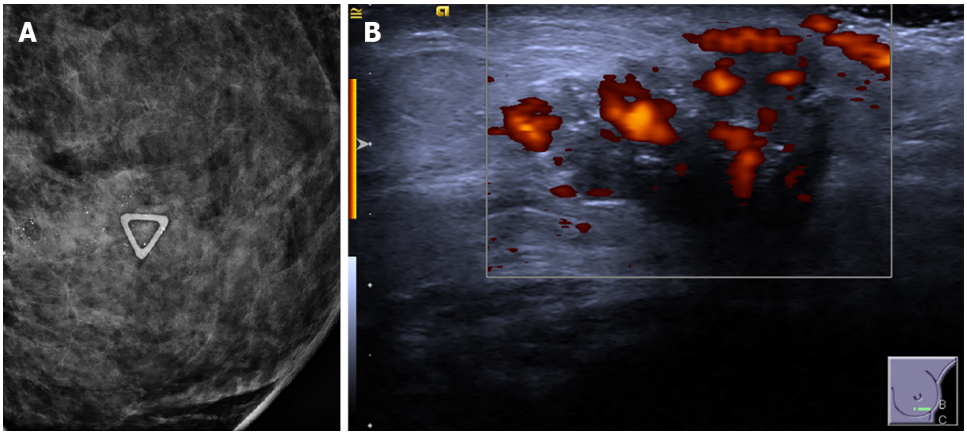

Figure 1 HER2-enriched invasive cancer. A: High-risk microcalcifications on mammogram of the left breast are seen within the palpable mass (denoted by triangular skin marker); B: Irregular hypoechoic mass showing increased internal vascularity (Adler Index Grade III) and internal echogenic foci representing microcalcifications.

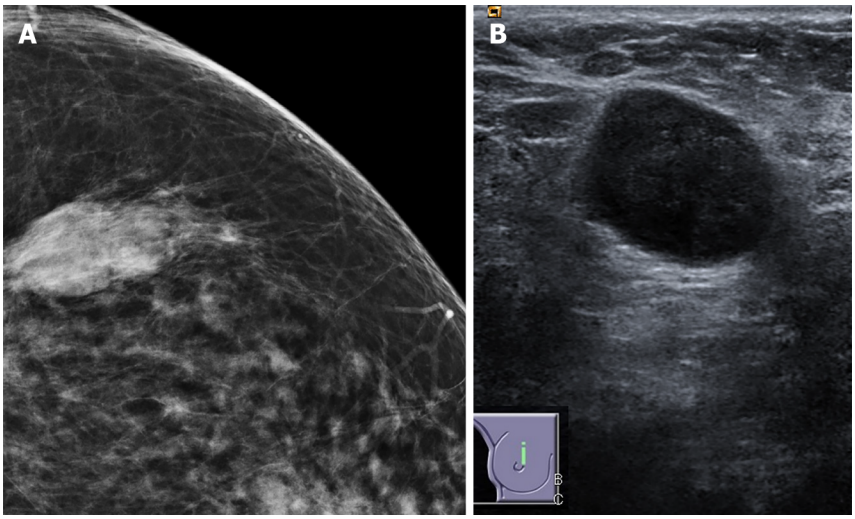

Figure 2 Triple negative breast cancer. A: Circumscribed mass on mammogram; B: Circumscribed hypoechoic mass with posterior acoustic enhancement on ultrasound.

cancer (n = 20, 15%). This was confirmed in the univariate binomial and multinomial regressions, posterior acoustic shadowing suggested a higher likelihood of the tumor being a hormone receptor positive type (univariate: P = 0.037, OR 4.26) (Table 3). However, there was no statistically significant positive association in the multivariate model specifications, possibly due to the lack of statistical power given the limited sample size.

Of the DCIS tumors that were visible on US (60% of all DCIS), the majority did not show any posterior acoustic features (n = 16, 51%). In comparison, most of the invasive cancers showed either posterior shadowing, enhancement, or a mix of both and only a minority showed no posterior acoustic features (n = 79, 29%). Absence of posterior acoustic features favors DCIS in the univariate and multivariate regressions (univariate: P = 0.028, OR 3.24; multivariate: P = 0.090, OR 2.49) (Table 6).

Vascularity

Tumors with a high score on the Adler index (II or III) comprised a minority of the sample (n = 55, 23%), and were more predominant in the HER2 enriched and TNBC subtypes (n = 21, 42%, n = 20, 42%, respectively) (Figure 1B). High vascularity was statistically significant as a predictor of HER2-enriched status in both the multivariate and univariate regressions (univariate regression: P = 0.011, OR 2.32; multivariate regression: P = 0.05, OR 1.99) (Table 5), while low vascularity is more likely in Luminal A tumors, corroborating similar findings in other studies[3] (Table 3). Similar to another study which showed a positive association between TNBC and high

vascularity using optoacoustic US imaging[7], we also found a positive association between TNBC cancers and vascularity in the univariate, but not multivariate specifications (univariate: $P = 0.022$, OR 2.12) (Table 4).

Tumor size

Tumor size was one of the strongest predictors of TNBC. If the lesion is large (> 20 mm), the relative odds of the tumor being a TNBC subtype would be 13 times higher compared to a non-TNBC type (univariate regression: $P \leq 0.001$, OR 13.20; Multivariate regression: $P \leq 0.001$, OR 10.54) (Table 4). In the multinomial regressions, large tumor size consistently predicted a higher likelihood of the tumor being TNBC *vs* all other subtypes. The high positive correlation between size and TNBC status reflects the fact that almost all the TNBC tumors were large ($n = 44$, 92%), compared to around 40% of the Luminal A/B tumors, and 60% of the HER2 enriched tumors. Large tumor size also signaled a higher likelihood of HER2-enriched status *vs* DCIS and Luminal A in the multinomial regression ($P = 0.008$, OR 3.73; $P = 0.05$, OR 1.97) (Table 7).

In contrast, sonographically visible DCIS and hormone receptor positive cancers are typically small (< 20 mm). In the univariate and multivariate regressions, small size increases the relative likelihood of the tumor being a DCIS type by 2.5-3 times, compared to invasive cancers (univariate: $P = 0.006$, OR 2.59; multivariate: $P = 0.012$, OR 3.02) (Table 6). Within the invasive cancer subtypes, a small sized tumor signals a higher likelihood of the tumor being either Luminal A/B (hormone receptor positive), compared to HER2-enriched or TNBC (univariate: $P \leq 0.001$, OR 4.26; multivariate: $P = 0.002$, OR 2.74) (Table 3).

Axillary node metastasis

Axillary node metastasis was most common in TNBC cancers ($n = 16$, 33%), followed by Luminal A ($n = 25$, 18%), and least prevalent in the Luminal B subtype ($n = 1$, 3%). We found evidence that TNBC is associated with a higher positive rate of axillary adenopathy compared to the non-TNBC tumors in the univariate binomial logistic regression ($P = 0.008$, OR 2.53) (TNBC *vs* non TNBC) but not the multivariate binomial logistic regression (Table 4). In the univariate multinomial model, the presence of axillary adenopathy represented a higher likelihood of the tumor being TNBC ($P = 0.029$, OR 18.50) or Luminal A subtype ($P = 0.043$, OR 3.08) relative to Luminal B subtype (Table 4). Our results are in keeping with several studies who also recorded a positive association between the presence of axillary node metastases and TNBC cancers[8,9]. However, the findings on axillary adenopathy and TNBC association have been mixed in the literature, with some other studies finding a negative association instead[10].

Multivariate logistic regressions

Although the univariate regressions show that a few key radiologic imaging features are statistically significant as independent prognostic indicators of the BC subtype, using a joint combination of imaging features could increase the reliability of the preliminary diagnosis. This is because US image acquisition is highly user dependent, and radiologic interpretation may sometimes be equivocal, for instance, in the case of lobulated (microlobulated) *vs* angular (spiculated) margins.

Similar to previous studies[7,11], we estimated multivariate binomial logistic regressions using the stepwise regression approach (SLE = 0.05, SLS = 0.05), with the final model specification determined by the Akaike information criterion. We catalogue four distinct categorizations: (1) Hormone-receptor positive *vs* hormone-receptive negative invasive cancers; (2) TNBC *vs* non-TNBC invasive cancers; (3) HER2-enriched *vs* non HER2-enriched invasive cancers; and (4) DCIS *vs* invasive cancers. The distinguishing characteristics for each category are: (1) A small lesion (< 20 mm), with spiculated margins, the absence of posterior acoustic enhancement and absence of high-risk microcalcifications, is more likely associated with hormone-receptor positive status (Figure 3); (2) Posterior acoustic enhancement, circumscribed margins, and large tumor size was predictive of TNBC status; (3) Microlobulated margins, high-risk microcalcifications, and high vascularity was predictive of HER2-enriched status; and (4) Absence of posterior acoustic features and small size on ultrasound was associated with DCIS compared to invasive cancers. A receiver operating characteristic curve was plotted using the pROC package in R; the performance of the multivariate models based on the AUC was (1) 0.792; (2) 0.853; (3) 0.747; and (4) 0.719, respectively.

Table 7 Multinomial univariate logistic regressions: Impact of imaging features on relative odds of molecular subtypes

			Luminal A baseline			Luminal B baseline			DCIS baseline			HER2 enriched baseline			TNBC baseline		
			P value	OR	95%CI	*P* value	OR	95%CI	*P* value	OR	95%CI	*P* value	OR	95%CI	*P* value	OR	95%CI
Posterior acoustic features	Shadowing	Luminal A *vs*							[d]	**3.27**	**(0.832 12.83)**	[b]	**7.35**	**(1.979 27.300)**			
		Luminal B *vs*										[a]	**7.50**	**(1.307 43.030)**			
		DCIS *vs*	[d]	0.31	(0.078 1.202)												
		HER2+ *vs*	[b]	0.14	(0.037 0.505)	[a]	0.13	(0.023 0.765)									
		TNBC *vs*															
	Enhancement	Luminal A *vs*													[b]	0.19	(0.055 0.633)
		Luminal B *vs*															
		DCIS *vs*													[a]	0.12	(0.024 0.610)
		HER2+ *vs*													[a]	0.22	(0.058 0.807)
		TNBC *vs*	[b]	**5.38**	**(1.581 18.310)**				[a]	**8.25**	**(1.638 41.55)**	[a]	**4.64**	**(1.239 17.38)**			
Margins (on US)	Spiculated	Luminal A *vs*				[a]	**2.45**	**(1.130 5.31)**	[b]	**5.41**	**(1.931 15.14)**	[c]	**5.88**	**(2.544 13.58)**	[c]	**4.26**	**(1.805 10.056)**
		Luminal B *vs*	[a]	0.41	(0.188 0.885)							[d]	**2.40**	**(0.861 6.690)**			
		DCIS *vs*	[b]	0.19	(0.066 0.518)												
		HER2+ *vs*	[c]	0.17	(0.074 0.393)	[d]	0.42	(0.150 1.16)									
		TNBC *vs*	[c]	0.24	(0.099 0.554)												
	Circumscribed	Luminal A *vs*													[b]	0.09	(0.019 0.445)
		Luminal B *vs*															
		DCIS *vs*															
		HER2+ *vs*															
		TNBC *vs*	[b]	**10.8**	**(2.246 52.043)**												
Size	Large	Luminal A *vs*										[a]	0.51	(0.258 0.999)	[c]	0.07	(0.024 0.208)
		Luminal B *vs*													[c]	0.08	(0.023 0.259)
		DCIS *vs*													[c]	0.04	(0.010 0.134)
		HER2+ *vs*	[a]	**1.97**	**(1.001 3.878)**										[c]	0.14	(0.043 0.450)
		TNBC *vs*	[c]	**14.20**	**(4.811 41.915)**	[c]	**12.94**	**(3.856 43.427)**	[c]	**26.89**	**(7.445 97.114)**	**c**	**7.21**	**(2.224 23.354)**			
High-risk	Present	Luminal							[c]	0.30	(0.154	[b]	0.34	(0.171			

Microcals		A *vs*								0.583)			0.665)			
		Luminal B *vs*						[d]	0.44	(0.186 1.061)						
		DCIS *vs*	[c]	**3.34**	**(1.715 6.488)**	[d]	**2.25**	**(0.942 5.37)**						[b]	**4.50**	**(1.606 9.96)**
		HER2+ *vs*	[b]	**2.97**	**(1.504 5.844)**									[b]	**4.00**	**(1.824 11.10)**
		TNBC *vs*						[b]	0.22	(0.090 0.548)		0.25	(0.100 0.623)			
Adler	High	Luminal A *vs*									[c]	0.27	(0.131 0.566)	[b]	0.30	(0.142 0.618)
		Luminal B *vs*														
		DCIS *vs*									[d]	0.38	(0.136 1.037)	[d]	0.41	(0.147 1.131)
		HER2+ *vs*	[c]	**3.68**	**(1.767 7.650)**			[d]	**2.67**	**(0.965 7.37)**						
		TNBC *vs*	[b]	**3.38**	**(1.618 7.045)**			[d]	**2.45**	**(0.884 6.78)**						
Axillary node adenopathy	Yes	Luminal A *vs*				[a]	**3.08**	**(1.063 61.96)**						[a]	0.44	(0.209 0.919)
		Luminal B *vs*	[a]	0.12	(0.224 0.470)						[a]	0.07	(0.009 0.556)	[b]	0.05	(0.007 0.430)
		DCIS *vs*														
		HER2+ *vs*				[a]	**14.40**	**(1.798 115.17)**								
		TNBC *vs*	[a]	**2.28**	**(1.088 4.778)**	[b]	**18.50**	**(2.323 147.34)**								

[a]Significant at the 0.001 level.
[b]Significant at the 0.01 level.
[c]Significant at the 0.05 level.
[d]Significant at the 0.10 level.
Only statistically significant results are shown. Bold results show higher relative odds. DCIS: Ductal carcinoma *in situ*; TNBC: Triple-negative breast cancer; US: Ultrasound.

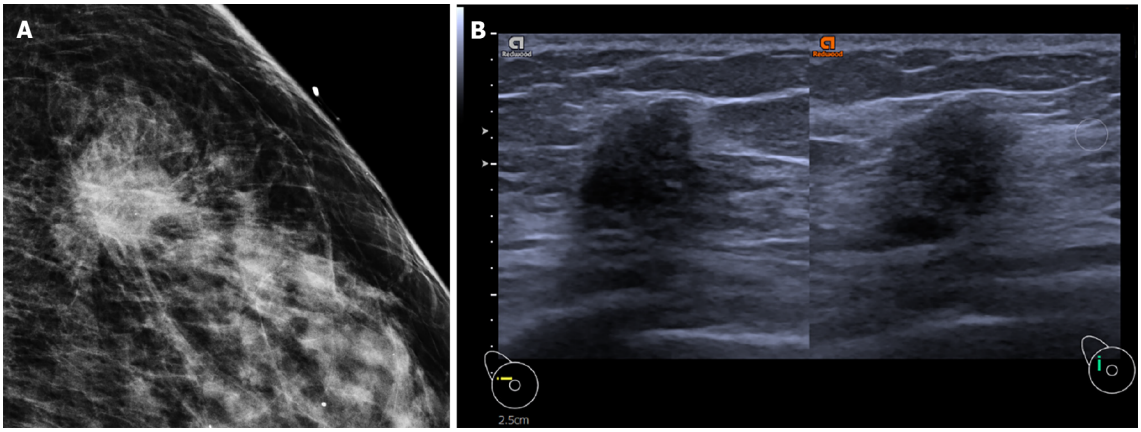

Figure 3 Luminal type invasive cancer. A: Spiculated mass on mammogram; B: Irregular hypoechoic mass with spiculated margin and posterior acoustic shadowing.

Screening and size of tumor

A significant proportion of the cancers in our sample were detected *via* routine breast screening (n = 91, 28%). Previous studies have shown that BCs detected *via* screening are typically smaller than symptomatic BCs, and that screening is an effective means of

detecting tumors at an earlier stage[12].

In our sample, screening detected tumors when they were smaller, even after controlling for molecular subtype. The mean size of hormone receptor negative tumors detected *via* screening was 19.0 mm *vs* 33.0 mm for hormone receptor negative cancers presenting with symptoms. The mean size of TNBC and HER2-enriched cancers that were detected *via* screening was 32.5 mm and 14.4 mm respectively *vs* 34.7 mm and 30.8 mm, respectively for symptomatic patients. However, as size is a less important predictor of disease severity than the biologic characteristics of the tumor based on its gene expression, a few prominent studies have downplayed the usefulness of breast screening in improving patient outcomes, considering its tendency for overdiagnosis of in-situ type cancers[13].

One of the main findings of our study is that TNBC cancers tend to have benign morphologic features, such as circumscribed margins and posterior enhancement. This raises possibility of mistaking it for common benign lesions such as cysts with echoes or fibroadenomas. The only unique differentiator is its positive correlation with size. Thus, in the screening context, size may be a useful factor in deciding whether to recommend an invasive biopsy or imaging follow-up for the lesion in question.

To estimate the impact of size on the probability of the tumor being a TNBC subtype conditional on the tumor presenting during screening, in the multivariate regressions, we specified an interaction term of screening with size, and find a marginally significant positive coefficient for the interaction term. Interpretively, this means that for every unit increase in lesion size, there are higher relative odds of the screening tumor being a TNBC subtype compared to non-TNBC, holding all other factors unchanged (P = 0.08, OR 1.18) (Table 4).

DISCUSSION

BC is a heterogenous disease, characterized by the varied imaging appearance, histologic and molecular profiles, and correspondingly different disease course across the various molecular subtypes. The different molecular types of BC have different biological behaviors at the cellular level, which influence the speed of invasion and destruction of the surrounding tissue, consequently affecting the macroscopic appearance of the tumor on mammogram and ultrasound.

Prior studies investigating the association of imaging features with molecular subtypes found evidence that cancers with posterior acoustic shadowing have higher odds of hormone-receptor positivity while those with posterior acoustic enhancement are likely to have negative receptor expression[14]. TNBC cancers were more likely to have circumscribed margins while hormone receptor positive cancers were more likely to show spiculated margins[15,16]. High risk microcalcifications detected on mammogram are associated with HER2-enriched cancers[17]. Our results are generally consistent with prior studies, with imaging features that correlate with the following subtypes: Spiculated margins were positively correlated with hormone receptor positive status (Luminal A or B). As hypothesized by earlier research, as luminal cancers tend to be lower grade and grow at a slower rate, they provoke a desmoplastic reaction, resulting in radiologic findings of spiculated margins. The desmoplastic reaction also affects acoustic impedance of the tumor to healthy tissue interface, causing excessive sonographic attenuation by the tumor, resulting in posterior shadowing[14,15,18].

High-risk microcalcifications, vascularity, and microlobulated margins, are positively associated with HER2 enriched cancers. Studies have shown that HER2 gene overexpression is linked to neo-angiogenesis *via* production of VEGF[19], while high-risk microcalcifications are due to the tendency of HER2 cancers to have a concomitant DCIS component[20]. Rapidly proliferating tumor cells, which consume the blood supply, lead to tumor necrosis and subsequent acidosis in the microenvironment, resulting in calcium accumulation in the ducts[21]. Our results concur with prior studies, which reported high risk microcalcifications to be more frequent in HER2+ tumors compared to luminal cancers[22].

A statistically significantly relationship exists between TNBC, which is the most aggressive molecular subtype, and posterior acoustic enhancement, circumscribed margins, and large tumor size. These are more cellular, grow rapidly, and do not generally incite a strong desmoplastic reaction from the surrounding healthy tissue[6]. The more regular interface between tumor and surrounding tissue probably results in a circumscribed margin, while internal necrosis and high cellularity probably attenuate the sound waves to a lesser degree, manifesting as posterior enhancement on

ultrasound. Concordant with other studies[8,11], US tumor size was a statistically significant predictor of TNBC cancers. In our sample, we found that if detected through breast screening (patients were asymptomatic), each unit increase in tumor size is associated with a higher odds ratio for TNBC cancer relative to the rest of the subtypes. This may imply that breast screening could be detecting TNBC at an earlier stage (smaller size, non-palpable), and that clinicians should prioritize biopsy of larger lumps when assessing screening populations.

DCIS is characterized by architectural distortions and high-risk microcalcifications on MG, but only 60% of DCIS tumors are visible on US (n = 31, 58%). High-risk microcalcifications tend to be absent in DCIS tumors that are sonographically visible. On US, a combination of small size and absence of posterior acoustic features favor DCIS. These two sonographic features are also commonly seen in benign lesions. However, similar to invasive cancers, the majority of sonographically visible DCIS show microlobulated or spiculated margins, whereas the overwhelming majority of benign lesions demonstrate circumscribed margins[23]. This highlights the importance of margin assessment of even small lesions on ultrasound, which depends on the skill of the performing technologist, as well as the use of a high-resolution probe.

In the current landscape of BC chemotherapeutic regimens, hormonal therapy is routinely used for hormone-receptor positive tumors (Luminal A/B), while targeted therapy, such as Herceptin, is available for cancers which overexpress HER2 (Luminal B/HER2-enriched). On the other hand, not only are TNBC tumors more aggressive (due to poor dedifferentiation), and have a higher recurrence rate, no targeted therapeutic strategy is currently available for the treatment of TNBC, leaving non-targeted chemotherapy as the only weapon in the chemotherapeutic arsenal. Stratification may allow for earlier resection times by aiding radiologists in deciding whether to biopsy or observe the lesion. As screening detects tumors at an earlier stage, large size is one discriminating feature that could point towards an aggressive TNBC subtype—prioritizing biopsy for these cases may benefit patient outcomes. In addition, histopathological analysis may not be readily available in certain developing countries, and an improved understanding of how the imaging features of BC correlate to molecular subtype would aid in tailoring the treatment strategy for patients who are cost constrained.

Our study had several limitations. First, as this was a retrospective study conducted at a single institution, it could have been subject to selection bias with respect to patients who arrive at our institution, even though we endeavored to minimize selection bias by including all consecutive patients within a fixed duration of time and blinding the assessing radiologists to the histology results. Second, due to the relatively small sample size, some of the subanalysis could have lacked statistical power to detect a significant difference in imaging features across molecular subtypes. Nevertheless, we see potential for further research, particularly in automated machine learning. From studies such as ours, imaging features identified as effective predictors could be used to customize deterministic algorithms for computer-extracted features, which could then be utilized at large-scale and with no inter-reader variability[2]. In fact, a recent study introduced a machine learning model for MRI classification of BC subtypes, guiding their radiomic feature selection and categorization by a review of the prior literature for imaging features that exhibited prognostic significance for various aspects of BC[24].

CONCLUSION

In conclusion, key features in mammographic and sonographic imaging were significantly associated with BC molecular subtypes. Knowledge of such correlations could help clinicians stratify BC patients according to their likely molecular subtype, potentially enabling earlier, more effective treatment or aiding in therapeutic decisions in countries where receptor testing is not readily available.

ARTICLE HIGHLIGHTS

Research background

There is evidence in the literature that breast cancer (BC) molecular subtypes often have characteristic imaging features on mammogram (MG), ultrasound (US) and magnetic resonance imaging. These imaging features on MG and US are of particular

interest as they are cost-effective and widely available even in many developing countries.

Research motivation

Thus far, research into the correlation between MG and US imaging features and BC subtypes has been based on populations of symptomatic patients, with the lack of data on an asymptomatic (screening) population highlighted as an area for future research. We wanted to thus use our data which consists of both screening and symptomatic patients to add to the body of knowledge on this issue. Also, our population includes patients with ductal carcinoma-in-situ (DCIS) which only a few papers have examined.

Research objectives

To correlate the MG and US imaging features with the molecular subtypes of BC (hormone receptor positive *vs* hormone receptor negative, triple-negative *vs* non-triple negative and HER2 positive *vs* HER2 negative) and DCIS in our population of screening and symptomatic patients.

Research methods

Our study is retrospective, with a population of 328 consecutive patients in 2017-18 with histologically confirmed BC. 237 (72%) were symptomatic, and 91 (28%) were detected *via* a screening program. All the patients underwent MG and US imaging prior to biopsy. The images were retrospectively interpreted by two breast-imaging radiologists with 5-10 years of experience who were blinded to the histology results to ensure statistical independence. To test the hypothesis that imaging features are correlated with tumor subtypes, univariate binomial and multinomial logistic regression models were performed. Also, multivariate logistic regression (with and without interaction terms) was utilized to identify combinations of MG and US imaging characteristics predictive of molecular subtypes.

Research results

Circumscribed margins, posterior enhancement, and large size are correlated with triple-negative BC (TNBC). High-risk microcalcifications and microlobulated margins is predictive of HER2-enriched cancers. DCIS is characterized by small size on US, absence of posterior acoustic features, and the presence of architectural distortion on MG. Hormone receptor positive subtypes tend to be small, with spiculated margins and posterior acoustic shadowing. These results are broadly consistent with findings from prior studies. In addition, we also find that US lesion size signals a higher odds ratio for TNBC if presented during screening.

Research conclusions

Several MG and US imaging features were shown to independently predict molecular subtypes of BC, in a population of both screening and symptomatic patients. Knowledge of such correlations could help clinicians stratify BC patients, possibly enabling earlier treatment for patients with triple negative cancer. This could also aid therapeutic decisions in countries where receptor testing is not readily available.

Research perspectives

To further research in this field, machine learning algorithms may be trained to recognize both the imaging characteristics as well as the radionomic characteristics of BC molecular subtypes, to see if this can further improve the predictive accuracy of imaging. More studies with asymptomatic populations of patients, and with differing ethnicities would also be useful to corroborate the results in our study.

REFERENCES

1 **Pinker K**, Chin J, Melsaether AN, Morris EA, Moy L. Precision Medicine and Radiogenomics in Breast Cancer: New Approaches toward Diagnosis and Treatment. *Radiology* 2018; **287**: 732-747 [PMID: 29782246 DOI: 10.1148/radiol.2018172171]

2 **Grimm LJ**, Mazurowski MA. Breast Cancer Radiogenomics: Current Status and Future Directions. *Acad Radiol* 2020; **27**: 39-46 [PMID: 31818385 DOI: 10.1016/j.acra.2019.09.012]

3 **Rashmi S**, Kamala S, Murthy SS, Kotha S, Rao YS, Chaudhary KV. Predicting the molecular subtype of breast cancer based on mammography and ultrasound findings. *Indian J Radiol Imaging* 2018; **28**: 354-361 [PMID: 30319215 DOI: 10.4103/ijri.IJRI_78_18]

4 Y. Estimation of Random Utility Models in R: The mlogit Package. *J Stat Softw* 2020; **95**: 1-41 [DOI:

10.18637/jss.v095.i11]
5 **Venables WN**, Ripley BD. Modern Applied Statistics with S. 4th ed. Springer: New York, 2018
6 **Robin X**, Turck N, Hainard A, Tiberti N, Lisacek F, Sanchez JC, Müller M. pROC: an open-source package for R and S+ to analyze and compare ROC curves. *BMC Bioinformatics* 2011; **12**: 77 [PMID: 21414208 DOI: 10.1186/1471-2105-12-77]
7 **Dogan BE**, Menezes GLG, Butler RS, Neuschler EI, Aitchison R, Lavin PT, Tucker FL, Grobmyer SR, Otto PM, Stavros AT. Optoacoustic Imaging and Gray-Scale US Features of Breast Cancers: Correlation with Molecular Subtypes. *Radiology* 2019; **292**: 564-572 [PMID: 31287388 DOI: 10.1148/radiol.2019182071]
8 **Li CY**, Zhang S, Zhang XB, Wang P, Hou GF, Zhang J. Clinicopathological and prognostic characteristics of triple- negative breast cancer (TNBC) in Chinese patients: a retrospective study. *Asian Pac J Cancer Prev* 2013; **14**: 3779-3784 [PMID: 23886182 DOI: 10.7314/apjcp.2013.14.6.3779]
9 **Dent R**, Trudeau M, Pritchard KI, Hanna WM, Kahn HK, Sawka CA, Lickley LA, Rawlinson E, Sun P, Narod SA. Triple-negative breast cancer: clinical features and patterns of recurrence. *Clin Cancer Res* 2007; **13**: 4429-4434 [PMID: 17671126 DOI: 10.1158/1078-0432.CCR-06-3045]
10 **He ZY**, Wu SG, Yang Q, Sun JY, Li FY, Lin Q, Lin HX. Breast Cancer Subtype is Associated With Axillary Lymph Node Metastasis: A Retrospective Cohort Study. *Medicine (Baltimore)* 2015; **94**: e2213 [PMID: 26632910 DOI: 10.1097/MD.0000000000002213]
11 **Tandon A**, Srivastava P, Manchanda S, Wadhwa N, Gupta N, Kaur N, Pant CS, Pal R, Bhatt S. Role of Sonography in Predicting the Hormone Receptor Status of Breast Cancer: A Prospective Study. *J Diagnostic Med Sonogr* 2017; **34**: 3-14 [DOI: 10.1177/8756479317721663]
12 **Jørgensen KJ**, Gøtzsche PC, Kalager M, Zahl PH. Breast Cancer Screening in Denmark: A Cohort Study of Tumor Size and Overdiagnosis. *Ann Intern Med* 2017; **166**: 313-323 [PMID: 28114661 DOI: 10.7326/M16-0270]
13 **Welch HG**, Prorok PC, O'Malley AJ, Kramer BS. Breast-Cancer Tumor Size, Overdiagnosis, and Mammography Screening Effectiveness. *N Engl J Med* 2016; **375**: 1438-1447 [PMID: 27732805 DOI: 10.1056/NEJMoa1600249]
14 **Irshad A**, Leddy R, Pisano E, Baker N, Lewis M, Ackerman S, Campbell A. Assessing the role of ultrasound in predicting the biological behavior of breast cancer. *AJR Am J Roentgenol* 2013; **200**: 284-290 [PMID: 23345347 DOI: 10.2214/AJR.12.8781]
15 **Çelebi F**, Pilancı KN, Ordu Ç, Ağacayak F, Alço G, İlgün S, Sarsenov D, Erdoğan Z, Özmen V. The role of ultrasonographic findings to predict molecular subtype, histologic grade, and hormone receptor status of breast cancer. *Diagn Interv Radiol* 2015; **21**: 448-453 [PMID: 26359880 DOI: 10.5152/dir.2015.14515]
16 **Boisserie-Lacroix M**, Macgrogan G, Debled M, Ferron S, Asad-Syed M, McKelvie-Sebileau P, Mathoulin-Pélissier S, Brouste V, Hurtevent-Labrot G. Triple-negative breast cancers: associations between imaging and pathological findings for triple-negative tumors compared with hormone receptor-positive/human epidermal growth factor receptor-2-negative breast cancers. *Oncologist* 2013; **18**: 802-811 [PMID: 23821326 DOI: 10.1634/theoncologist.2013-0380]
17 **Cen D**, Xu L, Li N, Chen Z, Wang L, Zhou S, Xu B, Liu CL, Liu Z, Luo T. BI-RADS 3-5 microcalcifications can preoperatively predict breast cancer HER2 and Luminal a molecular subtype. *Oncotarget* 2017; **8**: 13855-13862 [PMID: 28099938 DOI: 10.18632/oncotarget.14655]
18 **Algazzar MAA**, Elsayed EE-M, Alhanafy AM, Mousa WA. Breast cancer imaging features as a predictor of the hormonal receptor status, HER2neu expression and molecular subtype. *Egypt J Radiol Nucl Med* 2020; **51**: 93 [DOI: 10.1186/s43055-020-00210-5]
19 **Kumar R**, Yarmand-Bagheri R. The role of HER2 in angiogenesis. *Semin Oncol* 2001; **28**: 27-32 [PMID: 11706393 DOI: 10.1016/s0093-7754(01)90279-9]
20 **Liao N**, Zhang GC, Liu YH, Li XR, Yao M, Xu FP, Li L, Wu YL. HER2-positive status is an independent predictor for coexisting invasion of ductal carcinoma in situ of the breast presenting extensive DCIS component. *Pathol Res Pract* 2011; **207**: 1-7 [PMID: 21095069 DOI: 10.1016/j.prp.2010.08.005]
21 **Tse GM**, Tan PH, Cheung HS, Chu WC, Lam WW. Intermediate to highly suspicious calcification in breast lesions: a radio-pathologic correlation. *Breast Cancer Res Treat* 2008; **110**: 1-7 [PMID: 17674189 DOI: 10.1007/s10549-007-9695-4]
22 **Sun SS**, Zhang B, Zhao HM, Cao XC. Association between mammographic features and clinicopathological characteristics in invasive ductal carcinoma of breast cancer. *Mol Clin Oncol* 2014; **2**: 623-629 [PMID: 24940507 DOI: 10.3892/mco.2014.297]
23 **Stavros AT**, Thickman D, Rapp CL, Dennis MA, Parker SH, Sisney GA. Solid breast nodules: use of sonography to distinguish between benign and malignant lesions. *Radiology* 1995; **196**: 123-134 [PMID: 7784555 DOI: 10.1148/radiology.196.1.7784555]
24 **Saha A**, Harowicz MR, Grimm LJ, Kim CE, Ghate SV, Walsh R, Mazurowski MA. A machine learning approach to radiogenomics of breast cancer: a study of 922 subjects and 529 DCE-MRI features. *Br J Cancer* 2018; **119**: 508-516 [PMID: 30033447 DOI: 10.1038/s41416-018-0185-8]

Published by **Baishideng Publishing Group Inc**
7041 Koll Center Parkway, Suite 160, Pleasanton, CA 94566, USA
Telephone: +1-925-3991568
E-mail: bpgoffice@wjgnet.com
Help Desk: https://www.f6publishing.com/helpdesk
https://www.wjgnet.com